Geochemical Perspectives Letters

Apollo 15 green glass He-Ne-Ar signatures – In search for indigenous lunar noble gases

E. Füri[1*], L. Zimmermann[1], A.E. Saal[2]

OPEN ACCESS

doi: 10.7185/geochemlet.1819

Abstract

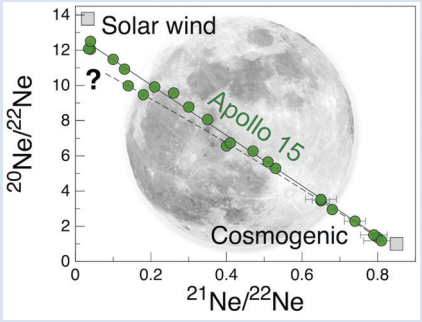

Identifying indigenous lunar noble gases in samples returned by the Apollo and Luna missions is highly challenging because contributions from the solar wind (SW) and/or cosmogenic nuclides have modified the noble gas signature of the regolith and rocks exposed to space at the lunar surface. Here we re-investigate the possible presence of indigenous noble gases in pyroclastic Apollo 15426 green glasses based on precise measurements of He-Ne-Ar isotopic compositions and abundances. The noble gas content of single glass beads varies by two orders of magnitude, indicating that they experienced highly variable irradiation histories as a result of intense regolith stirring by impact gardening. Four out of the twelve spherules stand out by having the highest He-Ne-Ar abundances and by releasing an isotopically 'solar-like' noble gas component at high temperatures. While a contribution from indigenous noble gases cannot be ruled out, the data are best accounted for by inward diffusion of, and equilibration with, SW-derived volatiles during prolonged space exposure.

Received 27 February 2018 | Accepted 23 July 2018 | Published 7 September 2018

Introduction

The recent discovery of indigenous water and other highly volatile elements (C, F, S, Cl; Saal *et al.*, 2008; Sharp *et al.*, 2010; Wetzel *et al.*, 2015) in samples returned by the Apollo missions demonstrates that the formation and evolution of the Moon involved processes that allowed for the accretion and retention of the most volatile elements in the Solar System. Although the source and timing of volatile accretion is still debated (Hauri *et al.*, 2015; Barnes *et al.*, 2016), these findings raise the question of whether the lunar mantle contains indigenous (*i.e.* primordial) noble gases that were supplied to the growing Moon by the delivery of volatile-rich chondritic matter or were inherited from the proto-Earth.

The isotopic and/or elemental abundance signature of indigenous lunar noble gases could provide crucial constraints on the origin and evolution of the Moon. However, indigenous lunar noble gases have never been unambiguously found despite extensive searches over the past five decades (Wieler and Heber, 2003), although recent high precision analyses hint at the presence of indigenous xenon in lunar anorthosites (Bekaert *et al.*, 2017). The key caveat is that noble gases of primordial origin can easily be masked by additional noble gas components. All rock and soil samples collected at the Moon's surface contain 'trapped' surface-correlated noble gases implanted by SW irradiation. Volume-correlated noble gases comprise cosmogenic nuclides (^{3}He, ^{21}Ne, ^{38}Ar) produced by spallation reactions, and radiogenic noble gases (^{4}He, ^{40}Ar) produced by the decay of long-lived radionuclides. Due to the modifications that occur during space exposure, discerning indigenous noble gases in currently available lunar samples is highly challenging.

Lakatos *et al.* (1973) proposed that green glass spherules from Apollo sample 15426 contain solar-like noble gases that may be of primordial origin. 15426 is a friable greenish clod that was collected by the Apollo 15 crew from the north rim of Spur Crater on the Apennine front. The green material is the common Apollo 15 very-low-Ti glass that was formed by volcanic fire-fountaining of primitive melts ~3.4 Gyr ago (Table S-1; Podosek and Huneke, 1973; Delano, 1979, 1986; Spangler *et al.*, 1984). Importantly, the presence of water, C, F, S, and Cl in the interior of the glass beads (Saal *et al.*, 2008; Wetzel *et al.*, 2015), together with the condensation and enrichment of volatile elements on the glass surface (Delano, 1979), requires the existence of a volatile-rich reservoir in the lunar mantle source.

Step-wise gas extraction, combined with multi-element isotope analysis, provides the only means for resolving noble gases into constituent components, and for detecting indigenous gas in lunar samples. Therefore, in this study, we re-assess the noble gas signature of 15426 green glasses by step-wise CO_2 laser extraction static mass spectrometry analysis (see Supplementary Information for details). Noble gas (He, Ne, Ar) concentrations and isotope ratios of twelve single vitreous glass beads, between 13 and 25 (±2) micrograms in mass,

1. Centre de Recherches Pétrographiques et Géochimiques, CNRS-UL, 15 rue Notre Dame des Pauvres, BP20, 54501 Vandoeuvre-lès-Nancy Cedex, France
2. Department of Geological Sciences, Brown University, Providence, RI 029112, USA
* Corresponding author (email: efueri@crpg.cnrs-nancy.fr)

were measured using the Helix MC *Plus* noble gas mass spectrometer at CRPG in Nancy, France. Two heating steps were applied: a low temperature step (~600 °C) allowed extracting surface-sited, thermally labile gases, whereas the fusion step (~1500 °C) was aimed at releasing volume-correlated, more refractory noble gas components. Since neon isotopes were measured in multi-collection mode on three electron multipliers, the analytical precision on neon isotope ratios has improved by a factor of two compared to our previous study of orange lunar volcanic glasses (Füri *et al.*, 2014). Such high precision measurements are key for distinguishing different noble gas components in lunar samples.

Noble Gas Signature of 15426 Green Glasses

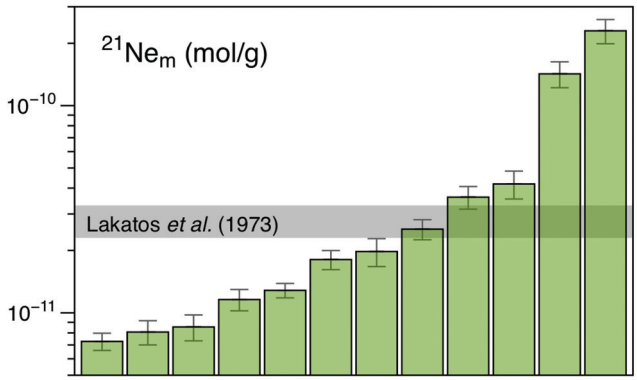

Figure 1 Total ^{21}Ne abundances of twelve single 15426 green glass beads. The uncertainty of 8 to 15 % is controlled by the precision in determining the sample mass. The ^{21}Ne concentration range reported by Lakatos *et al.* (1973) for five grain size fractions and two large single spherules is indicated for comparison.

The ^{4}He content of several 15426 spherules analysed here is below the detection limit, implying that the glasses experienced severe diffusive helium losses. Any remaining helium is predominantly released at the first heating step, and, in most cases, shows an isotope ratio comparable to that of modern SW (Table S-2). These results indicate that the glass beads contain surface-sited noble gases implanted by SW irradiation, with only minor remnants of radiogenic ^{4}He and cosmogenic ^{3}He in the grain interior. The neon and argon abundances vary by two orders of magnitude (Figs. 1 and 2d), and the concentration range recorded by the small 15426 green glass beads analysed here is significantly greater than that reported by Lakatos *et al.* (1973) for five grain size fractions and two large single spherules. ^{20}Ne/^{22}Ne and ^{21}Ne/^{22}Ne ratios vary between 12.50 and 1.18 and between 0.0350 and 0.815, respectively, and in a three-isotope plot of neon, most isotope signatures fall onto a mixing line between a high-^{20}Ne/^{22}Ne component (with ^{20}Ne/^{22}Ne = 12.42 ± 0.05 for ^{21}Ne/^{22}Ne = 0.03), interpreted to represent isotopically fractionated SW-derived neon, and cosmogenic neon (Fig. 2a). Similarly, ^{36}Ar/^{38}Ar ratios range from 5.51 to 0.91, also reflecting varying mixing proportions between SW-derived argon and a low-^{36}Ar/^{38}Ar cosmogenic component (Fig. 2b). The 'trapped' neon and argon component, implanted by SW irradiation, is predominantly released during the first heating step, whereas the cosmogenic isotopes are extracted during sample melting (Fig. 2). The solar gas component is isotopically depleted in the light neon isotopes compared to modern SW due to depth-dependent isotope fractionation upon implantation of SW and removal of surface-sited solar gas by ion sputtering (Wieler *et al.*, 2007). Importantly, four glass beads stand out by having the highest noble gas contents and by showing a distinct gas release pattern; *i.e.* four spherules release large amounts of SW-derived helium, neon, and argon at low temperatures, and a volume-correlated component with high ^{20}Ne/^{22}Ne, ^{36}Ar/^{38}Ar, and ^{36}Ar/^{22}Ne ratios is extracted at the second heating step (Fig. 2). In the three-isotope plot of neon, this end member falls below the mixing line defined by the other glass beads, and points to a ^{20}Ne/^{22}Ne ratio of 11.41 ± 0.04 (for ^{21}Ne/^{22}Ne = 0.03).

The lack of correlation between the noble gas abundance and the grain size (*i.e.* the surface/volume ratio) lead Lakatos *et al.* (1973) to propose that solar-like neon and argon in Apollo 15 green glasses may represent primordial lunar gas. However, the concentrations of 'trapped' solar neon and argon (Supplementary Information) found in 15426 glasses are several orders of magnitude greater than the Ne-Ar abundances in the 2ΠD43 popping rock, which is the least degassed terrestrial mid-ocean ridge basalt (Moreira *et al.*, 1998). Although an indigenous origin for noble gases in lunar volcanic glasses cannot be ruled out, it appears unlikely that i) lunar magmas escaped degassing, and ii) the lunar mantle contains a larger amount of neon and argon than the terrestrial upper mantle, given the Moon's general volatile element depletion compared to Earth (Hauri *et al.*, 2015). As an alternative to an indigenous origin, the melt that formed the 15426 green glasses may have assimilated SW-irradiated regolith upon eruption, resulting in dissolution of solar noble gases into the interior of the melt droplets before quenching (Lakatos *et al.*, 1973). Since lunar regolith contains 1.5 to 2 wt. % carbonaceous chondrite-like material (*e.g.*, Keays and Ganapathy, 1970), regolith assimilation should be detectable through analyses of highly siderophile elements (HSEs). Walker *et al.* (2004) argued that a significant proportion of chondritic HSEs is only present in the "etchate" of the surface of the green glasses, whereas concentrations are low in the residual glass. Another possibility is that the 15426 melt droplets trapped a gas phase that was released by heating and outgassing of vast quantities of solar wind-impregnated regolith (Lakatos *et al.*, 1973). However, it is difficult to envision how high noble gas partial pressures, allowing for the dissolution of inert gases into the erupting melt, could have been maintained during fire-fountain style eruptions in near vacuum at the lunar surface. In addition, rapid quenching of the erupting melt droplets must have prevented ingassing of volatiles released from the regolith.

In light of these caveats, the noble gas characteristics of the He-Ne-Ar-rich 15426 green glasses are best explained by inward diffusion of implanted SW-derived gas (with ^{20}Ne/^{22}Ne = 12.42 ± 0.05) – from the surface of the spherules into their interiors – during prolonged space exposure. When equilibrium conditions were established, the solar gases became volume- as opposed to surface-correlated (Lakatos *et al.*, 1973). Upon CO_2 laser heating, the diffusive gas release fractionates the ^{20}Ne/^{22}Ne ratio according to:

$$R_{residual} = R_{initial} \times f^{(1-\alpha)} \qquad \text{Eq. 1}$$

where $R_{initial}$ is the initial (solar-like) ^{20}Ne/^{22}Ne ratio, f is the fraction of neon remaining in the glass, and α is the isotope fractionation factor, which can be approximated by $\sqrt{m_{20}/m_{22}}$ for mass dependent fractionation. Since ~90 % of the total amount of neon was extracted from the two gas-richest spherules during the first heating step (*i.e.* f = 0.1; Table S-2), the cumulative fraction of neon released at low temperature is expected to record an integrated ^{20}Ne/^{22}Ne ratio of 12.05, whereas the residual 'trapped' neon is estimated to yield a ^{20}Ne/^{22}Ne ratio of 11.2; both estimates are in excellent agreement with the values observed here (Fig. 2a and Table S-2).

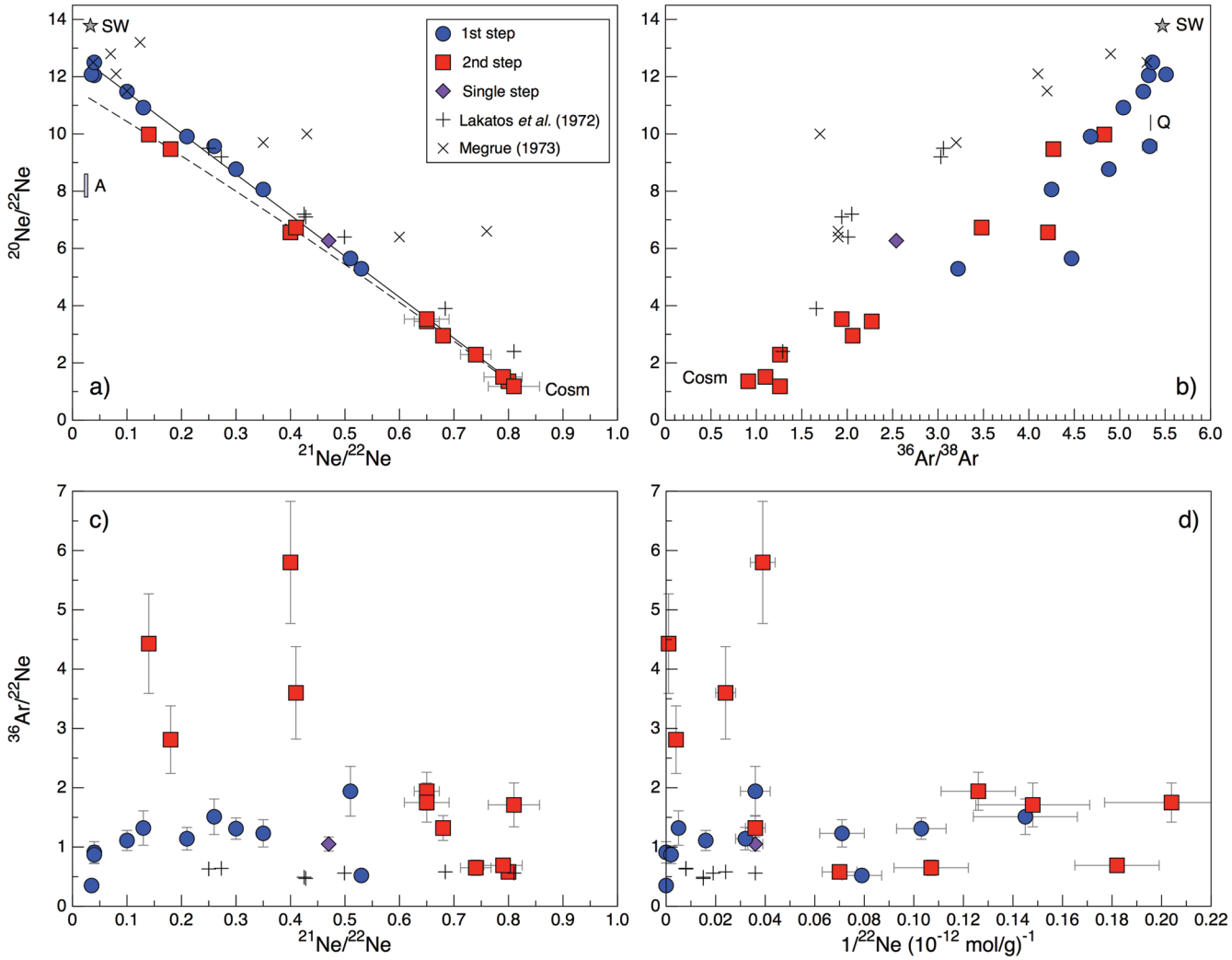

Figure 2 **(a)** Three-isotope plot of neon, **(b)** $^{20}Ne/^{22}Ne$ *versus* $^{36}Ar/^{38}Ar$, **(c)** $^{36}Ar/^{22}Ne$ *versus* $^{21}Ne/^{22}Ne$, and **(d)** $^{36}Ar/^{22}Ne$ *versus* the inverse of the ^{22}Ne concentration measured in 15426 green glasses. Step-heating data for single glass beads from this study are shown together with results obtained by single-step heating of different grain size fractions and two large single spherules (Lakatos *et al.*, 1973) and by laser ablation of individual spherules (Megrue, 1973). The neon and argon isotope compositions of the cosmogenic endmember (Cosm), modern solar wind (SW; Heber *et al.*, 2009), and the meteoritic components A and Q (Ott, 2014) are shown for comparison. Error bars for the results from this study represent 1σ uncertainties and are, in some cases, smaller than symbol sizes.

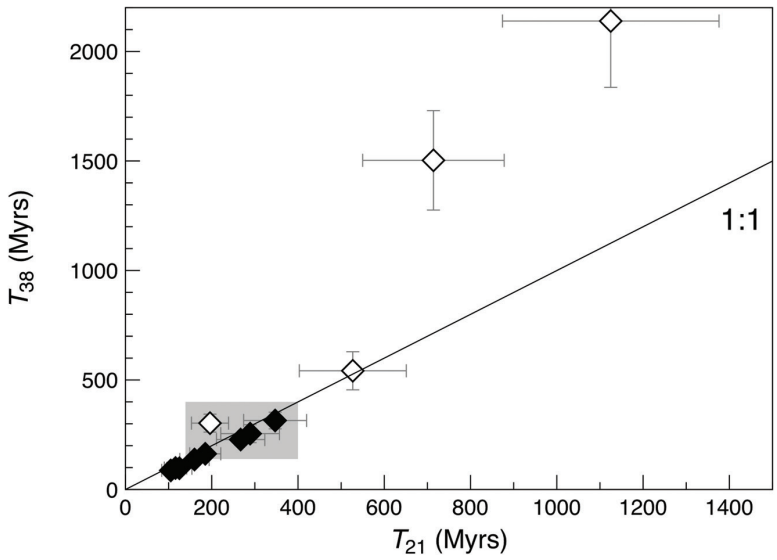

Figure 3 Cosmic ray exposure ages derived from the $^{21}Ne_{cosm}$ (T_{21}) and $^{38}Ar_{cosm}$ (T_{38}) concentrations. Data for the four He-Ne-Ar-rich 15426 glass beads (open diamonds) and eight other spherules (filled diamonds) are shown together with the CRE ages determined previously (grey rectangle; Huneke *et al.*, 1973; Lakatos *et al.*, 1973; Megrue, 1973; Spangler *et al.*, 1984).

Irradiation History of 15426 Green Glasses

Since the 15426 glass beads contain a binary mixture of SW-derived and cosmogenic ^{20,21,22}Ne and ^{36,38}Ar, the amount of $^{21}Ne_{cosm}$ and $^{38}Ar_{cosm}$ can be derived numerically for each sample, based on the isotopic signature of the two end members (see Supplementary Information for details on the component deconvolution). The concentrations of cosmogenic ^{21}Ne and ^{38}Ar correspond to cosmic ray exposure (CRE) ages (T_{21} and T_{38}, respectively) that agree within uncertainties, and vary between 87 ± 9 and 347 ± 73 Myr in most cases (Fig. 3 and Table 1). These CRE ages are comparable to the values of 139 to 400 Myr obtained by previous noble gas analyses of 15426 green glasses (Huneke *et al.*, 1973; Lakatos *et al.*, 1973; Megrue, 1973; Spangler *et al.*, 1984). However, three out of the four gas-rich glass beads clearly stand out by having high concentrations of cosmogenic ^{21}Ne and ^{38}Ar, reflecting extremely high exposure ages (T_{38}) between 542 ± 87 and 2139 ± 303 Myr (Fig. 3 and Table 1). This indicates that these spherules were exposed to cosmic, and possibly solar wind, irradiation at the (sub-) surface of the Moon for a much longer duration than the majority of the Apollo 15 green glasses which could have resulted in inward diffusion of SW-derived gases, facilitated by radiation damage. At the same time, diffusive loss of $^{21}Ne_{cosm}$ likely occurred, thus severely affecting the T_{21} exposure ages. These observations demonstrate that, due to intense stirring of the regolith by impact gardening, each individual lunar volcanic glass bead records its own unique irradiation history, which is accessible only through single grain analyses.

Table 1 Abundances of cosmogenic ^{21}Ne and ^{38}Ar and corresponding cosmic ray exposure ages of twelve single 15426 green glass beads.

Sample ID	$^{21}Ne_{cosm}$ (pmol/g)	% total	T_{21} (Myr)	$^{38}Ar_{cosm}$ (pmol/g)	% total	T_{38} (Myr)
15426-4	7.1	97	105 ± 21	3.7	59	87 ± 9
15426-11	7.8	96	116 ± 26	4.2	52	98 ± 14
15426-2	8.3	98	125 ± 29	4.2	64	97 ± 15
15426-5	10.7	92	160 ± 34	5.9	41	137 ± 17
15426-I	12.4	97	185 ± 36	7.0	62	163 ± 15
15426-13*	13.1	36	196 ± 43	13.0	9	303 ± 41
15426-II	17.9	99	267 ± 56	9.8	87	228 ± 26
15426-10	19.4	98	289 ± 68	11.0	51	255 ± 41
15426-6	23.2	92	347 ± 73	13.5	44	315 ± 38
15426-12*	35.3	84	527 ± 124	23.3	25	542 ± 87
15426-III*	47.8	34	714 ± 164	64.6	10	1503 ± 227
15426-3*	75.4	33	1125 ± 251	92.0	10	2139 ± 303

The four glass beads with the highest He-Ne-Ar abundances (Table S-2) are identified by asterisks.
Uncertainties for the $^{21}Ne_{cosm}$ and $^{38}Ar_{cosm}$ concentrations are on the order of 10 to 15 %.

In Search of Indigenous Lunar Noble Gases

The hydrogen (and nitrogen) isotopic signature of lunar samples is currently best explained by late accretion of volatile-rich chondritic material to the Moon, although the possibility that some volatiles were inherited from the proto-Earth cannot be ruled out (*e.g.*, Füri *et al.*, 2014; Hauri *et al.*, 2015; Barnes *et al.*, 2016). Could indigenous lunar noble gases provide further constraints on the origin of volatiles in the lunar interior, and, thus, on the formation and evolution of the Moon? Noble gas elemental ratios must have been fractionated throughout the volatile accretion process(es) by the Moon and/or upon partial melting and degassing during magmatic eruption; thus they are unlikely to preserve the original source characteristics. Noble gas isotope ratios represent excellent volatile source tracers; nonetheless identifying a chondritic or terrestrial provenance may be highly challenging because secondary contributions from the SW and/or cosmogenic nuclides hamper the identification of the indigenous component.

The terrestrial mantle is characterised by ^{20}Ne/^{22}Ne and ^{36}Ar/^{38}Ar ratios of 12.65 and 5.3, respectively (Péron *et al.*, 2017); thus, transfer of noble gases from Earth to the Moon-forming material would have resulted in isotope compositions that are very similar to those of the 'trapped' component in Apollo 15426 green glasses. SW-irradiated chondritic dust – with a high surface/volume ratio – would be characterised by comparable noble gas isotope signatures; however small dust grains can be ruled out as the dominant contributors to the lunar volatile inventory on the basis of predominantly non-solar hydrogen and nitrogen isotope signatures of Apollo samples. For large chondritic bodies, the neon inventory is dominated by neon in presolar diamonds (Ne-A), whereas the argon budget is dominated by the Q component. These end members are characterised by ^{20}Ne/^{22}Ne and ^{36}Ar/^{38}Ar ratios of ~8.2 and 5.34, respectively (Fig. 2a,b; Ott, 2014). Therefore, step-heating neon extraction, combined with precise isotope analysis by state-of-the-art static vacuum mass spectrometry, would allow a distinction between a chondritic and a terrestrial provenance of lunar volatiles. Although high-precision (He-)Ne-Ar data can now be obtained for very small (≤25 μg) lunar volcanic glasses, new lunar samples are needed to detect a possible indigenous noble gas component, and to identify unambiguously its provenance. Pristine samples that have never been exposed to space at the lunar surface, *i.e.* rock samples retrieved by drilling from depths of several metres or fresh crater ejecta, are key for assessing whether the lunar mantle retains indigenous noble gases that were supplied to the growing Moon by the delivery of volatile-rich chondritic matter were inherited from the proto-Earth.

Acknowledgements

We thank two anonymous reviewers for their constructive comments. This work was supported by the European Research Council (grant no. 715028 to E.F.). This is CRPG-CNRS contribution 2601.

Editor: Cin-Ty Lee

Additional Information

Supplementary Information accompanies this letter at http://www.geochemicalperspectivesletters.org/article1819.

Cite this letter as: Füri, E., Zimmermann, L., Saal, A.E. (2018) Apollo 15 green glass He-Ne-Ar signatures – In search for indigenous lunar noble gases. *Geochem. Persp. Let.* 8, 1–5.

References

Barnes, J.J., Kring, D.A., Tartèse, R., Franchi, I.A., Anand, M., Russell, S.S. (2016) An asteroidal origin for water in the Moon. *Nature Communications* 7, 11684.

Bekaert, D.V., Avice, G., Marty, B., Henderson, B., Gudipati, M.S. (2017) Stepwise heating of lunar anorthosites 60025, 60215, 65315 possibly reveals an indigenous noble gas component on the Moon. *Geochimica et Cosmochimica Acta* 218, 114–131.

Delano, J.W. (1979) Apollo 15 green glass: Chemistry and possible origin. *Proceedings of the 10th Lunar and Planetary Science Conference*, 275–300.

Delano, J.W. (1986) Pristine lunar glasses: criteria, data, and implications. Proceedings of the 16th Lunar and Planetary Science Conference, Part 2. *Journal of Geophysical Research* 91, D201–D213.

Füri, E., Deloule, E., Gurenko, A., Marty, B. (2014) New evidence for chondritic lunar water from combined D/H and noble gas analyses of single Apollo 17 volcanic glasses. *Icarus* 229, 109–120.

Hauri, E.H., Saal, A.E., Rutherford, M.J., Van Orman, J.A. (2015) Water in the Moon's interior: Truth and consequences. *Earth and Planetary Science Letters* 409, 252–264.

Heber, V.S., Wieler, R., Baur, H., Olinger, C., Friedmann, T.A., Burnett, D.S. (2009) Noble gas composition of the solar wind as collected by the Genesis mission. *Geochimica et Cosmochimica Acta* 73, 7414–7432.

Huneke, J.C., Podosek, F.A., Wasserburg, G.J. (1973) An argon bouillabaisse including ages from the Luna 20 site. *Abstracts of the Lunar and Planetary Science Conference* 4, 403–404.

Keays, R.R., Ganapathy, R. (1970) Trace elements and radioactivity in lunar rocks. Implications for meteorites infall, solar-wind flux, and formation conditions of Moon. *Science* 167, 490–493.

Lakatos, S., Heymann, D., Yaniv, A. (1973) Green spherules from Apollo 15: Inferences about their origin from inert gas measurements. *The Moon* 7, 132–148.

Megrue, G.H. (1973). Distribution of gases within Apollo 15 samples: implications for the incorporation of gases within solid bodies of the Solar System. *Journal of Geophysical Research* 78, 4875–4883.

Moreira, M., Kunz, J., Allègre, C. (1998) Rare gas systematics in Popping rock: Isotopic and elemental compositions in the upper mantle. *Science* 279, 1178-1181.

Ott, U. (2014) Planetary and pre-solar noble gases in meteorites. *Chemie der Erde - Geochemistry* 74, 519–544.

Péron, S., Moreira, M., Putlitz, B., Kurz, M.D. (2017) Solar wind implantation supplied light volatiles during the first stage of Earth accretion. *Geochemical Perspective Letters* 3, 151–159.

Podosek, F.A., Huneke, J.C. (1973) Argon in Apollo 15 green glass spherules (15426): ^{40}Ar-^{39}Ar age and trapped argon. *Earth and Planetary Science Letters* 19, 413–421.

Saal, A.E., Hauri, E.H., Lo Cascio, M., Van Orman, J.A., Rutherford, M.C., Cooper, R.F. (2008) Volatile content of lunar volcanic glasses and the presence of water in the Moon's interior. *Nature* 454, 192–195.

Sharp, Z.D., Shearer, C.K., McKeegan, K.D., Barnes, J.D., Wang, Y.Q. (2010). The chlorine isotope composition of the moon and implications for an anhydrous mantle. *Science* 329, 1050–1053.

Spangler, R.R., Warasila, R., Delano, J.W. (1984) ^{39}Ar-^{40}Ar ages for the Apollo 15 green and yellow glasses. Proceedings of the 14th Lunar and Planetary Science Conference, Part 2, *Journal of Geophysical Research* 89, B487–B497.

Walker, R.J., Horan, M.F., Shearer, C.K., Papike, J.J. (2004) Low abundances of highly siderophile elements in the lunar mantle: evidence for prolonged late accretion. *Earth and Planetary Science Letters* 224, 399–413.

Wetzel, D.T., Hauri, E.H., Saal, A.E., Rutherford, M.J. (2015) Carbon content and degassing history of the lunar volcanic glasses. *Nature Geoscience* 8, 755–758.

Wieler, R., Heber, V.S. (2003) Noble gas isotopes on the Moon. *Space Science Reviews* 106, 197–210.

Wieler, R., Grimberg, A., Heber, V.S. (2007) Consequences of the non-existence of the "SEP" component for noble gas geo-and cosmochemistry. *Chemical Geology* 244, 382–390.

Geochemical Perspectives Letters

Apollo 15 green glass He-Ne-Ar signatures - In search for indigenous lunar noble gases

E. Füri, L. Zimmermann, A.E. Saal

Supplementary Information

The Supplementary Information includes:

- Major Element Composition of 15426 Green Glasses
- Noble Gas (He, Ne, Ar) Analysis
- Noble Gas Component Deconvolution and Exposure Ages
- Figures S-1 and S-2
- Tables S-1 and S-2
- Supplementary Information References

Major Element Composition of 15426 Green Glasses

Green glasses collected during the Apollo 15 mission represent quenched picritic (17 to 19 wt. % MgO), very-low-Ti (0.2 to 0.4 wt. % TiO_2) melts, which explosively erupted ~3.4 Gyrs ago by fire-fountaining (*e.g.*, Podosek and Huneke, 1973; Delano, 1979, 1986; Spangler *et al.*, 1984; Steele *et al.*, 1992). They are among the most primitive material yet collected on the Moon (Green and Ringwood, 1973). The green glasses can be divided into discrete compositional groups, which were formed in distinct magmatic events and/or from different source regions (Delano, 1979; Steele *et al.*, 1992).

Table S-1 Average major element composition (in wt. %) of the five compositional groups A-E of Apollo 15426/27 very-low-Ti green glasses.

	Group A	Group B	Group C	Group D	Group E
SiO_2	45.10	46.57	48.17	45.35	45.37
Al_2O_3	7.37	7.62	7.44	7.16	7.15
MgO	17.07	17.65	18.30	17.78	18.41
MnO	0.26	0.26	0.26	0.26	0.26
CaO	8.39	8.51	8.36	8.25	8.04
FeO	19.87	18.74	16.80	20.65	20.33
Na_2O	0.13	0.14	0.11	0.13	0.14
K_2O	0.03	0.03	0.02	0.03	0.03
TiO_2	0.37	0.38	0.23	0.40	0.42
P_2O	0.02	0.03	0.02	0.03	0.03
Cr_2O_3	0.54	0.55	0.58	0.54	0.53
Total	99.14	100.46	100.28	100.59	100.69

Given the small size and mass of the 15426 glass beads studied here, the glasses have not been polished, and their major element composition could not be determined prior to noble gas analyses. However, major element compositions of 15426/27 green glasses were obtained by analyses of over two hundred individual beads using the Cameca SX100 electron microprobe at the Department of Geological Sciences, Brown University (Saal *et al.*, 2008; Wetzel *et al.*, 2015); average compositions for the five compositional groups A-E defined by Delano (1979) are reported in Table S-1.

Noble Gas (He, Ne, Ar) Analysis

Helium, neon, and argon abundances and isotope ratios were determined by CO_2 laser extraction static mass spectrometry (Humbert *et al.*, 2000; Hashizume and Marty, 2004). Twelve 15426 green glass beads, between 13 and 25 (± 2) μg in mass (Table S-2), were loaded into different pits of the laser chamber connected to the purification line of the Helix MC *Plus* (Thermofisher Scientific) noble gas mass spectrometer at the CRPG noble gas analytical facility (Fig. S-1). The sample chamber was pumped to ultra high vacuum and kept at a temperature of 120 °C for ~15 hours. After leaving the samples under high vacuum ($P \leq 10^{-8}$ Torr) for several days prior to analysis, they were heated individually with a continuous-mode infrared CO_2 laser mounted on an *x*-*y* stage. Two heating steps were applied by modulating the power of the laser and monitoring the heating procedure on a TV screen using a CCD camera. A low-temperature step (~600 °C) allowed extracting surface-sited (solar) gases, whereas the fusion step (~1500 °C) was aimed at releasing volume-correlated (cosmogenic, radiogenic, indigenous) noble gas components. The extracted noble gases were purified using five hot (500 °C) and cold (room temperature) Ti sponge getters. Argon was separated from helium and neon by adsorption onto a charcoal finger at 77 K, and helium and neon were subsequently trapped onto a He-cooled cryogenic trap at 15 K. Helium was first released from this trap at 34 K and analysed in peak-jumping mode (^{4}He on the H2 Faraday detector, ^{3}He on the central (Ax) compact discrete dynode (CDD) detector). Neon was released from the cryogenic trap by increasing the temperature to 110 K, and the amount of gas introduced into the mass spectrometer was reduced (to between 50 and 60% of the total amount of neon) through volume dilution in the volume-calibrated purification line (Fig. S-2). The three isotopes of neon were analysed in multi-collection mode (^{22}Ne on H1 CDD, ^{21}Ne on Ax CDD, ^{20}Ne on L2 CDD). Neon isotope analyses consisted of 5 blocks of 30 cycles, and peak centering was performed at the start of each measurement block. Furthermore, a charcoal finger at 77 K and a Zr-Al getter at room temperature were used to minimize the contribution of doubly charged ^{40}Ar and CO_2 to the ^{20}Ne and ^{22}Ne signals, respectively. Given the high mass resolution of the Helix MC *Plus* ($m/\Delta m \approx 1800$), $^{40}Ar^{++}$ is partially resolved from the peak of interest (Honda *et al.*, 2015; Zhang *et al.*, 2016); therefore, no correction was applied to the ^{20}Ne signal. The CO_2^+ signal was measured at the beginning of each neon analysis, and the ^{22}Ne signal was corrected using a CO_2^{++}/CO_2^+ ionization ratio of 0.4 %; notably, the contribution of CO_2^{++} to the ^{22}Ne signal amounted to only ~1 cps, and is therefore negligible. After releasing argon from the charcoal finger, the argon isotopes were analysed in peak-jumping mode (^{40}Ar on the central Faraday detector, ^{38,36}Ar on Ax CDD).

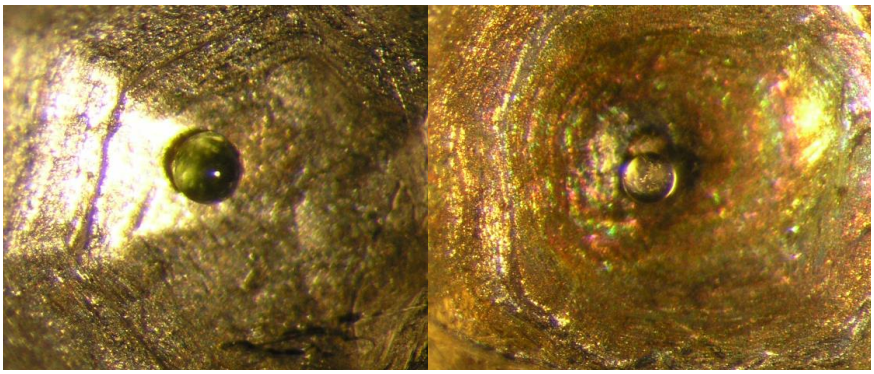

Figure S-1 Glass spherules in laser chamber pits before (left) and after (right) CO_2 laser heating. All glass spherules turned from green to colourless by heating to high temperature.

Air aliquots were used to determine the analytical sensitivity and reproducibility for neon and argon, whereas standard HESJ (He Standard of Japan) of Matsuda *et al.* (2002) with a ^{3}He/^{4}He ratio of 20.63 ± 0.10 R_A (where R_A is the atmospheric ^{3}He/^{4}He ratio) was used as a helium standard. The reproducibility (1σ s.d.) of standard measurements was 4 % for helium and 1 % for neon and argon abundances, whereas the reproducibility of the isotopic ratios ^{20}Ne/^{22}Ne, ^{21}Ne/^{22}Ne, and ^{36}Ar/^{38}Ar was 0.2 %, 0.6 %, and 0.4 %, respectively. Nonetheless, given the very small sample masses analysed here, uncertainties on noble gas concentrations (per gram of sample) are controlled by the precision of the weighing scale (*i.e.* ±2 μg) and are on the order of 8 to 15 %. Procedural blanks,

with the laser off, averaged 2.5 × 10^{-16} mol ^{20}Ne and 2.1 × 10^{-17} mol ^{36}Ar. Helium blanks were below the detection limit. Blank-corrected He-Ne-Ar abundances and isotope ratios for the twelve single 15426 green glass beads are given in Table S-2. Heating steps for which the blank contribution to the measured neon and abundances represents ≥25 % are reported in italics.

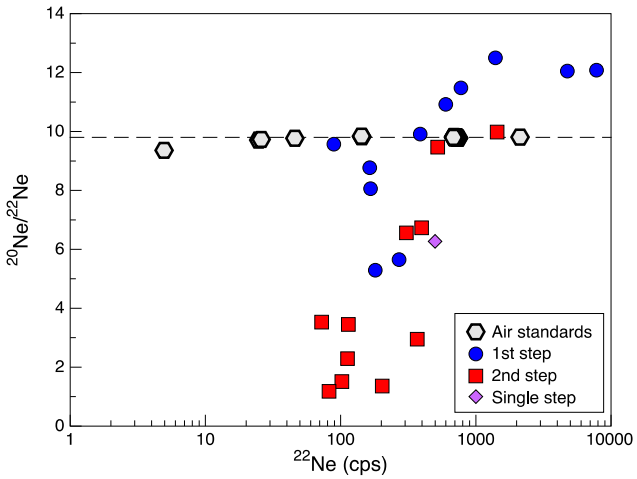

Figure S-2 ^{20}Ne/^{22}Ne ratios (corrected for instrumental mass discrimination) as a function of the ^{22}Ne signals (in counts per second, cps) for air standards and Apollo 15426 green glasses analysed by step-wise heating. The variable count rates for the air standard measurements were obtained by varying the amount of gas introduced into the mass spectrometer through volume dilution in the volume-calibrated purification line. The horizontal dashed line indicates the ^{20}Ne/^{22}Ne ratio of the terrestrial atmosphere (= 9.80 ± 0.08; *e.g.*, Porcelli *et al.*, 2002). Uncertainties (1σ s.d.) are smaller than symbol sizes.

Noble Gas Component Deconvolution and Exposure Ages

For lunar samples that contain a binary mixture between cosmogenic neon and 'trapped' neon implanted by solar wind (SW) irradiation, *i.e.* (^{21,22}Ne$_m$ = ^{21,22}Ne$_{cosm}$ + ^{21,22}Ne$_{tr}$), the amount of cosmogenic ^{21}Ne can be derived from

$$(^{21}Ne)_{cosm} = {}^{22}Ne_m \times \left(\frac{^{21}Ne}{^{22}Ne}\right)_{cosm} \frac{\left(\frac{^{21}Ne}{^{22}Ne}\right)_{tr} - \left(\frac{^{21}Ne}{^{22}Ne}\right)_{m}}{\left(\frac{^{21}Ne}{^{22}Ne}\right)_{tr} - \left(\frac{^{21}Ne}{^{22}Ne}\right)_{cosm}} \qquad \text{Eq. S-1}$$

where (^{22}Ne)$_m$ and (^{21}Ne/^{22}Ne)$_m$ are the measured ^{22}Ne abundances and ^{21}Ne/^{22}Ne ratios, respectively. (^{21}Ne/^{22}Ne)$_{cosm}$ is the cosmogenic neon endmember and (^{21}Ne/^{22}Ne)$_{tr}$ represents trapped SW-derived neon. Neon in the SW has a ^{20}Ne/^{22}Ne and ^{21}Ne/^{22}Ne ratio of 13.78 ± 0.03 and 0.0329 ± 0.0001, respectively (Table S-2; Heber *et al.*, 2009). However, neon implanted into lunar samples by SW irradiation has a significantly lower ^{20}Ne/^{22}Ne value of 11.2 to 12.8 (Grimberg *et al.*, 2006; Péron *et al.*, 2017), consistent with the data obtained here for 15426 green glasses (^{20}Ne/^{22}Ne$_{tr}$ = 12.42 ± 0.05; Fig. 2a). The distinct isotope composition results from both the depth-dependent isotope fractionation upon implantation of SW due to the higher energies and greater penetration depths of heavier isotopes – as demonstrated by Grimberg *et al.* (2006) for the implantation of SW neon into a Genesis target – and the removal of near-surface-sited SW gas by ion sputtering (Wieler *et al.*, 2007; Raquin and Moreira, 2009). In contrast, the neon isotopic signature of the cosmogenic endmember depends on the chemical composition of the sample and the irradiation conditions (*i.e.* solar (SCR) versus galactic cosmic rays (GCR); shielding depth); the (^{21}Ne/^{22}Ne)$_{cosm}$ ratio of mare basalts varies between 0.8 and 0.9 (*e.g.*, Füri *et al.*, 2015), and an average (^{21}Ne/^{22}Ne)$_{cosm}$ value of 0.93 has been reported by Leya *et al.* (2001) for the lunar regolith. Since the irradiation conditions of 15426 green glasses are unknown, and the major element composition of the glass beads studied here has not been determined, we use the lowest (0.035) and highest (0.815) ^{21}Ne/^{22}Ne values measured in our samples for the trapped and cosmogenic endmembers, respectively.

Similarly, the concentration of cosmogenic ^{38}Ar is obtained from

$$(^{38}Ar)_{cosm} = {}^{38}Ar_m \times \frac{\left(\frac{^{36}Ar}{^{38}Ar}\right)_{tr} - \left(\frac{^{36}Ar}{^{38}Ar}\right)_{m}}{\left(\frac{^{36}Ar}{^{38}Ar}\right)_{tr} - \left(\frac{^{36}Ar}{^{38}Ar}\right)_{cosm}} \qquad \text{Eq. S-2}$$

where $(^{38}Ar)_m$ and $(^{36}Ar/^{38}Ar)_m$ are the measured ^{38}Ar abundances and $^{36}Ar/^{38}Ar$ ratios, respectively, $(^{36}Ar/^{38}Ar)_{cosm}$ is the cosmogenic Ar component (≈ 0.7; Hohenberg *et al*., 1978), and $(^{36}Ar/^{38}Ar)_{tr}$ represents trapped SW-derived Ar. SW Ar is characterised by a $^{36}Ar/^{38}Ar$ ratio of 5.47 ± 0.02 (Heber *et al.*, 2009), whereas trapped, surface-correlated Ar in lunar soils generally has a lower isotope ratio of ~5.2 to 5.35 (*e.g.*, Bogard and Hirsch, 1978). The gas-richest sample in this study yields a $^{36}Ar/^{38}Ar$ ratio of 5.51 ± 0.02 at the first heating step; this value is adopted here for trapped argon.

Based on the two-component model, we estimate that for eight out of the twelve glass beads, ≥92 % of the total ^{21}Ne content has been produced in situ by cosmic ray induced spallation reactions during space exposure (Table 1), and the amount of cosmogenic ^{38}Ar represents between 41 and 87 % of the total ^{38}Ar content. The four spherules with the highest measured He-Ne-Ar abundances contain ~33 to 84 % ^{21}Ne of cosmogenic origin with a small fraction (~9 to 25 %) of $^{38}Ar_{cosm}$. Accordingly, the abundance of trapped ^{22}Ne varies between 5 and 61 ($\times 10^{-12}$) mol/g for eight beads, whereas the four gas-rich spherules record $^{22}Ne_{tr}$ concentrations between 189 and 4480 ($\times 10^{-12}$) mol/g. While this trapped component is predominantly extracted at the first heating step – consistent with surface implantation by the SW – the gas-rich glasses release up to 617 ($\times 10^{-12}$) mol$^{22}Ne_{tr}$/g upon sample melting.

The abundance of cosmogenic nuclides in lunar samples depends on the duration of exposure to cosmic rays and the production rates, which themselves are a function of the chemical composition and the irradiation conditions. Given that the lunar regolith is stirred to considerable depths by meteorite impacts, individual soil grains are unlikely to have acquired all their cosmogenic nuclides at a constant depth. Here, we estimate the cosmic ray exposure (CRE) ages by adopting an average production rate for the top 100 g/cm^2 of shielding, and by assuming that contributions from SCRs are negligible. Neon isotope production rates by SCRs are significantly higher than those by GCRs at the uppermost lunar surface (*e.g.*, by a factor ~20 for ^{20}Ne; Hohenberg *et al*., 1978); thus, any contribution of SCR-derived neon is expected to result in a noticeable shift of the $^{21}Ne/^{22}Ne$ ratio to lower values than observed here (≤0.75; Füri *et al.*, 2017). Based on the 2π exposure model of Leya *et al.* (2001), the production rate of cosmogenic ^{21}Ne by GCRs is on the order of 6.7 ± 1.2 ($\times 10^{-14}$) mol(g rock)$^{-1}$ Ma^{-1}, using an averaged composition for the Apollo 15 green glasses (Table S-1). The production rate of cosmogenic ^{38}Ar is less well known (Füri *et al*., 2017). The numerical model of Hohenberg *et al.* (1978) yields a value of 2.5 ± 0.7 ($\times 10^{-14}$) mol(g rock)$^{-1}$ Ma^{-1} for the green glasses, but it significantly underestimates the noble gas nuclide production rates compared to the model of Leya *et al.* (2001). Empirical $^{38}Ar_{cosm}$ production rates from Bogard *et al.* (1971) and Spangler *et al.* (1984) range from 4.1 to 4.5 ($\times 10^{-14}$) mol(g rock)$^{-1}$ Ma^{-1}. We use here the latter values, as they yield CRE ages (T_{38}) that agree, in most cases, within uncertainties with those derived from the $^{21}Ne_{cosm}$ (T_{21}) concentrations (Table 1). We note, however, that new physical models are crucially needed to reliably determine the depth-dependent production rates of cosmogenic argon isotopes in 2π exposure geometries by GCRs.

Table S-2 Helium, neon, and argon abundances and isotope ratios of twelve single Apollo 15426 green glass beads. The isotopic composition of solar wind (Heber *et al.*, 2009), chondritic (*i.e.* A, Q; Busemann *et al.*, 2000, and references therein), and terrestrial (Stuart *et al.*, 2003; Yokochi and Marty, 2004; Péron *et al.*, 2017) noble gases are given for comparison.

Sample ID	Mass (µg)	^{3}He	^{4}He	^{3}He/^{4}He (×10^{-4})	^{20}Ne	^{21}Ne	^{22}Ne	^{20}Ne/^{22}Ne	^{21}Ne/^{22}Ne	^{36}Ar	^{38}Ar	^{40}Ar	^{36}Ar /^{38}Ar
15426-I	25	7.7	3.87	20.0 ± 1.2	174.3	12.8	28.0	6.27 ± 0.02	0.467 ± 0.004	29.3	11.37	*294*	2.54 ± 0.02
15426-II-1	19	2.3	b.d.		65.8	6.7	12.6	5.29 ± 0.02	0.535 ± 0.007	6.6	2.11	b.d.	3.22 ± 0.04
15426-II-2		0.6	b.d.		*17.8*	11.4	14.3	1.36 ± 0.02	0.800 ± 0.012	8.4	9.20	*136*	0.91 ± 0.01
15426-III-1	14	44.1	104.95	4.2 ± 0.2	30368.0	91.9	2520.2	12.05 ± 0.04	0.0370 ± 0.0003	2305.0	436.88	8641	5.32 ± 0.02
15426-III-2		1.9	b.d.		2608.9	50.5	275.7	9.47 ± 0.03	0.184 ± 0.001	775.9	182.41	2367	4.27 ± 0.02
15426-3-1	15	55.6	133.93	4.2 ± 0.2	46605.0	132.9	3863.0	12.08 ± 0.04	0.0350 ± 0.0003	1334.8	243.78	9960	5.51 ± 0.02
15426-3-2		7.5	21.74	3.5 ± 0.2	7088.9	96.7	709.7	9.98 ± 0.03	0.138 ± 0.001	3146.8	650.63	5553	4.83 ± 0.02
15426-2-1	14	4.8	b.d.		*65.5*	1.7	6.9	9.57 ± 0.04	0.257 ± 0.003	10.4	1.90	*71*	5.33 ± 0.08
15426-2-2		5.7	b.d.		*19.8*	6.8	9.3	2.29 ± 0.03	0.738 ± 0.028	6.0	4.66	*197*	1.26 ± 0.02
15426-4-1	21	5.4	b.d.		84.5	2.9	9.7	8.77 ± 0.03	0.301 ± 0.004	12.8	2.58	*54*	4.88 ± 0.04
15426-4-2		0.9	b.d.		*7.2*	4.4	5.5	1.51± 0.04	0.795 ± 0.035	3.8	3.71	*111*	1.10 ± 0.02
15426-5-1	17	3.5	8.60	4.1 ± 0.3	306.1	6.4	31.0	9.91 ± 0.03	0.209 ± 0.002	35.4	7.46	*272*	4.68 ± 0.03
15426-5-2		0.2	b.d.		*26.1*	5.2	7.9	3.45 ± 0.03	0.651 ± 0.023	15.4	6.83	*276*	2.27 ± 0.02
15426-6-1	18	6.0	12.72	4.7 ± 0.3	702.6	6.0	61.0	11.48 ± 0.04	0.100 ± 0.001	67.7	12.85	*969*	5.26 ± 0.02
15426-6-2		2.7	b.d.		82.2	19.3	28.0	2.95 ± 0.04	0.684 ± 0.008	36.9	17.98	*419*	2.06 ± 0.01
15426-11-1	15	3.9	4.67	8.3 ± 0.6	112.9	4.9	14.0	8.06 ± 0.03	0.351 ± 0.005	17.3	3.78	*166*	4.25 ± 0.07
15426-11-2		0.3	b.d.		*16.5*	3.2	*4.9*	3.53 ± 0.05	0.654 ± 0.041	8.6	4.36	*278*	1.94 ± 0.03
15426-10-1	13	13.3	3.51	37.7 ± 9.3	156.1	14.2	27.9	5.65 ± 0.02	0.509 ± 0.007	53.9	12.15	*583*	4.47 ± 0.02
15426-10-2		b.d.	b.d.		*6.3*	5.6	*6.8*	1.18 ± 0.05	0.815 ± 0.047	11.5	9.42	*275*	1.26 ± 0.01
15426-13-1	16	42.4	95.01	4.5 ± 0.3	8191.8	25.7	653.0	12.50 ± 0.04	0.0396 ± 0.0003	566.6	105.56	4395	5.36 ± 0.02
15426-13-2		1.6	5.83	2.7 ± 0.3	170.1	10.5	25.9	6.56 ± 0.02	0.404 ± 0.005	150.3	35.95	*665*	4.21 ± 0.02
15426-12-1	13	30.3	65.04	4.7 ± 0.3	2087.6	24.5	190.4	10.92 ± 0.03	0.130 ± 0.001	252.0	50.07	1805	5.04 ± 0.02
15426-12-2		4.3	12.32	3.5 ± 0.3	284.0	17.4	42.1	6.73 ± 0.02	0.413 ± 0.004	151.4	43.76	*1225*	3.48 ± 0.02

Table S-2 Cont.

Sample ID	Mass (µg)	^{3}He	^{4}He	^{3}He/^{4}He (×10^{-4})	^{20}Ne	^{21}Ne	^{22}Ne	^{20}Ne/^{22}Ne	^{21}Ne/^{22}Ne	^{36}Ar	^{38}Ar	^{40}Ar	^{36}Ar /^{38}Ar
Solar wind				4.64 ± 0.09				13.78 ± 0.03	0.0329 ± 0.0001				5.47 ± 0.01
Q				1.23 ± 0.02				10.11 to 10.67	0.0294 ± 0.0010				5.34 ± 0.02
A				1.35 to 1.55				8.2 ± 0.4	0.025 ± 0.003				5.3 ± 0.1
Earth				≥ 1.26				12.65 to 13.0					5.3

b.d.: below detection limit. Gas extraction steps for which the blank contribution represents ≥25 % are given in italics.
Concentration of ^{4}He in 10^{-9} mol/g, concentrations of ^{3}He, ^{20,21,22}Ne, and ^{36,38,40}Ar in 10^{-12} mol/g.
Uncertainties on noble gas concentrations are on the order of 8 to 15 % for the largest and smallest sample masses, respectively.

Supplementary Information References

Bogard, D.D., Funkhouser, J.G., Schaeffer, O.A., Zähringer, J. (1971) Noble gas abundances in lunar material - Cosmic-ray spallation products and radiation ages from the Sea of Tranquility and the Ocean of Storms. *Journal of Geophysical Research 76*, 2757–2779.

Bogard, D.D., Hirsch, W.C. (1978) Depositional and irradiational history and noble gas contents of orange-black droplets in the 74002/1 core from Shorty Crater. *Proceedings of the 9th Lunar and Planetary Science Conference*, 1981–2000.

Busemann, H., Baur, H., Wieler, R. (2000) Primordial noble gases in "phase Q" in carbonaceous and ordinary chondrites studied by closed-system stepped etching. *Meteoritics and Planetary Science* 35, 949–973.

Delano, J.W. (1979) Apollo 15 green glass: Chemistry and possible origin. *Proceedings of the 10th Lunar Science Conference*, 275–300.

Delano, J.W. (1986) Pristine lunar glasses: criteria, data, and implications. Proceedings of the 16th Lunar and Planetary Science Conference, Part 2, *Journal of Geophysical Research* 91, D201–D213.

Füri, E., Barry, P.H., Taylor, L.A., Marty, B. (2015) Indigenous nitrogen in the Moon: Constraints from coupled nitrogen–noble gas analyses of mare basalts. *Earth and Planetary Science Letters* 431, 195–205.

Füri, E., Deloule, E., Trappitsch, R. (2017) The production rate of cosmogenic deuterium at the Moon's surface. *Earth and Planetary Science Letters* 474, 76–82.

Green, D.H., Ringwood, A.E. (1973) Significance of a primitive lunar basaltic composition present in Apollo 15 soils and breccias. *Earth and Planetary Science Letters* 19, 1–8.

Grimberg, A., Baur, H., Bochsler, P., Bühler, F., Burnett, D.S., Hays, C.C., Heber, V.S., Jurewicz, A.J.G., Wieler, R. (2006) Solar wind neon from Genesis: implications for the lunar noble gas record. *Science* 314, 1133–1135.

Hashizume, K., Marty, B. (2004) Nitrogen isotopic analyses at the sub-picomole level using an ultra-low blank laser extraction technique. In: de Groot, P.A. (Ed.) *Handbook of stable isotope analytical techniques*. Elsevier Science, Amsterdam, 361–375.

Heber, V.S., Wieler, R., Baur, H., Olinger, C., Friedmann, T.A., Burnett, D.S. (2009) Noble gas composition of the solar wind as collected by the Genesis mission. *Geochimica et Cosmochimica Acta* 73, 7414–7432.

Hohenberg, C.M., Marti, K., Podosek, F.A., Reedy, R.C., Shirck, J.R. (1978) Comparison between observed and predicted cosmogenic noble gases in lunar samples. *Proceedings of the 9th Lunar and Planetary Science Conference*, 2311–2344.

Honda, M., Zhang, X., Phillips, D., Hamilton, D., Deerberg, M., Schwieters, J.B. (2015) Redetermination of the ^{21}Ne relative abundance of the atmosphere, using a high resolution, multi-collector noble gas mass spectrometer (HELIX-MC *Plus*). *International Journal of Mass Spectrometry* 387, 1–7.

Humbert, F., Libourel, G., France-Lanord, C., Zimmermann, L., Marty, B. (2000) CO_2-laser extraction-static mass spectrometry analysis of ultra-low concentrations of nitrogen in silicates. *Geostandard Newsletters* 24, 255–260.

Leya, I., Neumann, S., Wieler, R., Michel, R. (2001) The production of cosmogenic nuclides by galactic cosmic-ray particles for 2π exposure geometries. *Meteoritics and Planetary Science* 36, 1547–1561.

Matsuda, J., Matsumoto, T., Sumino, H., Nagao, K., Yamamoto, J., Miura, Y., Kaneoka, I., Takahata, N., Sano, Y. (2002) The ^{3}He/^{4}He ratio of the new internal He Standard of Japan (HESJ). *Geochemical Journal* 36, 191–195.

Péron, S., Moreira, M., Putlitz, B., Kurz, M.D. (2017) Solar wind implantation supplied light volatiles during the first stage of Earth accretion. *Geochemical Perspective Letters* 3, 151–159.

Podosek, F.A., Huneke, J.C. (1973) Argon in Apollo 15 green glass spherules (15426): ^{40}Ar-^{39}Ar age and trapped argon. *Earth and Planetary Science Letters* 19, 413–421.

Porcelli D., Ballentine C.J., Wieler, R. (2002) An overview of noble gas geochemistry and cosmochemstry. In: Porcelli, D., Ballentine, C.J., Wieler, R. (Eds.) *Noble gases in Geochemistry and Cosmochemistry*. Reviews in Mineralogy and Geochemistry, vol. 47. Mineral. Soc. Am., Washington, DC, 1-18.

Raquin, A., Moreira, M. (2009) Atmospheric ^{38}Ar/^{36}Ar in the mantle: Implications for the nature of the terrestrial parent bodies. *Earth and Planetary Science Letters* 287, 551-558.

Saal, A.E., Hauri, E.H., Lo Cascio, M., Van Orman, J.A., Rutherford, M.C., Cooper, R.F. (2008) Volatile content of lunar volcanic glasses and the presence of water in the Moon's interior. *Nature* 454, 192–195.

Spangler, R.R., Warasila, R., Delano, J.W. (1984) ^{39}Ar-^{40}Ar ages for the Apollo 15 green and yellow glasses. Proceedings of the 14th Lunar and Planetary Science Conference, Part 2, *Journal of Geophysical Research* 89, B487–B497.

Steele, A.M., Colson, R.O., Korotev, R.L., Haskin, L.A. (1992) Apollo 15 green glass: Compositional distribution and petrogenesis. *Geochimica et Cosmochimica Acta* 56, 4075–4090.

Stuart, F.M., Lass-Evans, S., Fitton, J.G., Ellam, R.M. (2003) High ^{3}He/^{4}He ratios in picritic basalts from Baffin Island and the role of a mixed reservoir in mantle plumes. *Nature* 424, 57–9.

Wetzel, D.T., Hauri, E.H., Saal, A.E., Rutherford, M.J. (2015) Carbon content and degassing history of the lunar volcanic glasses. *Nature Geoscience* 8, 755–758.

Wieler, R., Grimberg, A., Heber, V.S. (2007) Consequences of the non-existence of the "SEP" component for noble gas geo-and cosmochemistry. *Chemical Geology* 244, 382–390.

Yokochi, R., Marty, B. (2004) A determination of the neon isotopic composition of the deep mantle. *Earth and Planetary Science Letters* 225, 77–88.

Zhang, X., Honda, M., Hamilton, D. (2016) Performance of the High Resolution, Multi-collector Helix MC Plus Noble Gas Mas Spectrometer at the Australian National University. *Journal of The American Society of Mass Spectrometry* 27, 1937–1943.